

TRANSVERSE SINGLE PARTICLE INSTABILITY IN THE NAL 500 GeV ACCELERATOR

R. Stiening and E.J.N. Wilson†
National Accelerator Laboratory, Batavia, U.S.A.

Abstract

Experiments reveal that single particle resonances, driven by field imperfections limit the 8 GeV acceptance of the NAL main accelerator to protons with betatron oscillation amplitudes less than 8 mm. It is observed that resonances driven by random azimuthal field fluctuations are much weaker than those driven by average field errors acting in concert with the super-periodicity of the accelerator. This consideration dictates the choice of operating tune. Correction magnets are installed to compensate zero harmonic skew quadrupole, sextupole and octupole errors. Separate control of dv_x/dp , dv_y/dp , d^2v_x/dp^2 , and d^2v_y/dp^2 is possible in an energy-dependent manner. High azimuthal harmonic patterns correction magnets are used to eliminate, dipole, quadrupole, sextupole and skew sextupole resonances adjacent to the operating point. A description of these systems and the improvements obtained are given.

1. Introduction

The NAL main ring is fed with twelve batches of 8 GeV protons delivered at 15 Hz repetition rate by the fast cycling booster. These are loaded head to tail to fill the circumference of the main ring and during the loading sequence which lasts 0.8 seconds the main ring must act as a d.c. storage ring. Once the loading is complete the guide field rises parabolically until, at about 20 GeV, the maximum acceleration rate is reached and sustained to full energy.

Soon after this injection scheme was first implemented it became clear that a considerable fraction of the injected beam was lost during the loading sequence. Each batch decayed exponentially with a time constant of less than 1 second and this loss continued during the parabola, tailing off to zero near 20 GeV (Fig. 1). The fraction of the injected beam which survived to full energy was rarely higher than 35% and the peak intensity was limited to 10^{12} protons per pulse.

Improvements in the intensity delivered by the booster, which inevitably resulted in a larger transverse emittance, did little to raise the high energy intensity but merely augmented the losses.

Preliminary experiments showed that switching off the r.f. did not affect the loss rate nor was the loss diminished on those days when the brightness of the injected beam was low. This suggested that the loss

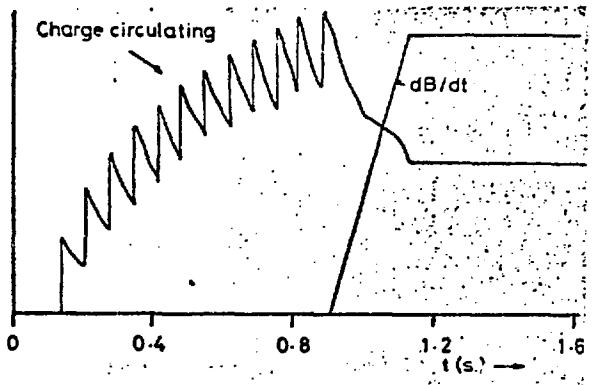


FIG.1 Loss during main ring loading and parabola

was due to a transverse single particle acceptance limitation rather than a longitudinal or collective phenomenon.

The acceptance limitation seemed not to be a purely mechanical obstruction. Measurements of beam profile and the closed orbit distortion after correction revealed that the beam occupied only a 20 mm diameter central core of the 100 mm x 50 mm section vacuum chamber. Moreover, one could bump the beam locally at any point in the machine almost to the vacuum chamber wall before any mechanical obstacle killed the beam.

On the other hand we found that the loss rate was very sensitive to the current in the main quadrupoles of the FODO lattice which affect the tune (ν_x, ν_y) and to the strength of the sextupole magnets which had been installed to reduce the large chromatic time spread in the injected beam.

We suspected that there were strong resonance lines in the working diamond driven by non linear imperfections in the guide field and that these were responsible for the losses. We therefore commenced a program of studies, which included improvements in techniques for measuring betatron motion and the installation of multipole correction magnets, with the intention of compensating the non linearities and reducing the tune spread in the beam. The remainder of this report describes this work which, at the time of writing, has improved the main ring to the point that it will accept and accelerate over 10^{13} protons per pulse rejecting under the best conditions only 10 to 20% of the beam presented by the booster.

† Visitor from CERN.

NOTICE

This report was prepared as an account of work sponsored by the United States Government. Neither the United States nor the United States Atomic Energy Commission, nor any of their employees, nor any of their contractors, subcontractors, or their employees, makes any warranty, express or implied, or assumes any legal liability or responsibility for the accuracy, completeness or usefulness of any information, apparatus, product or process disclosed, or represents that its use would not infringe privately owned rights.

2. Exploration of the NAL Working Diamond

Figure 2 shows the position of the nominal injection tune of the main ring in relation to the more important resonance lines. The lines are excited by random azimuthal variations in the non linear imperfections in the guide field.

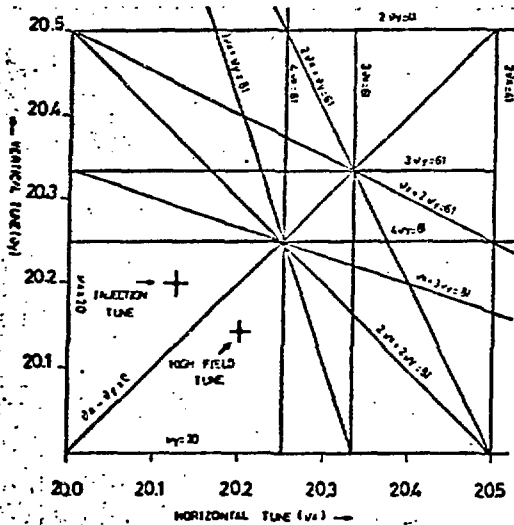


FIG 2. Working diagram.

The F and D sets of main ring quadrupoles are connected in series but are powered independently of the dipoles. By changing the ratio of quadrupole to bending magnet current we were able to scan the working point along a line $\nu_x - \nu_y = -0.08$, parallel to the diagonal coupling resonance $\nu_x - \nu_y = 0$. The small difference in the tunes is due to guide field imperfections. The configuration of the F and D quadrupole bus bars allowed us to shunt a small fraction of the current from the F to the D system through a pulsed vacuum tube power supply: the tune splitter. In this way we were able to control the tune split, $\nu_x - \nu_y$, and scan along a variety of lines mapping the working diamond at injection.

We calibrated these manipulations of the F and D quadrupole currents against measurements made by kicking the beam with a "pinger" dipole. This consisted of two turns of copper pulsed within a machine revolution from a small capacitor bank. By injecting a single booster batch and photographing an oscilloscope trace of the signal from one of the standard capacitive beam position detectors one could examine the beat frequency of the coherent betatron oscillations and calculate the fractional part of ν_x or ν_y , dividing the number of beats by the number of machine revolutions. We also deduced the tune spread in the beam from the rate of decay of the coherent signal and from the vertical oscillations induced by a radial kick could measure coupling between the two planes. We did not feel we could entrust disentangling these three signatures to a more convenient automated process at this stage.

Since we were interested in the influence of the resonances on beam loss we measured the fraction of the beam surviving by sampling and digitising a beam intensity monitor just after the injection of a single booster batch and again 400 milliseconds later. This quantity, the transmission, we measured with steady 8 GeV magnet excitation and with the r.f. switched on. It proved to be a powerful probe in exposing the resonance lines and reliable index of the overall transmission of the main ring to high energy.

We were fortunate in that we were able to make these injection studies parasitically with a special booster batch injected each machine cycle before the main batch sequence destined for acceleration to high energy.

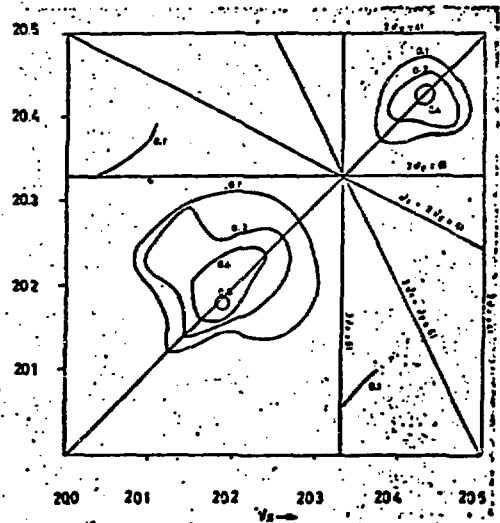


FIG 3. Contours of transmission for 0.4 sec at 8 GeV with original air cored sextupole pattern.

Figure 3 shows a contour plot obtained at the outset of these studies by measuring 8 GeV transmission as a function of ν_x and ν_y . Clearly the influence of the resonance lines extends over the whole working space and there is no one place where more than 70% of the beam survives.

Beam survival is best close to the diagonal coupling resonance $\nu_x - \nu_y = 0$. But in this region there is a danger that this coupling will transfer a large horizontal emittance into the vertical plane and our method of ν measurement became confused. One of the first corrections applied was to compensate the skew quadrupole imperfections the guide field which drive this coupling.

3. Correction of Skew Quadrupole Coupling

Coupling between vertical and horizontal phase planes can be driven by systematic skew quadrupole imperfections in the guide field such as might result if all the quadrupoles of one type were rotated by a fraction of a milliradian about the beam axis. An

average roll of this magnitude could quite easily creep in during the surveying of the ring but could be compensated by rolling a few quadrupoles in the opposite sense. Significant coupling is to be expected in a region centred on the line $v_x - v_y = 0$, of width:

$$v_x - v_y = \frac{1}{2(8s)} \int_0^c \sqrt{6_x^2 s_y} \, kds$$

where: k is the skew quadrupole $\partial B_x/\partial x$, $\partial B_y/\partial y$
 B_0 , the magnetic rigidity
 $6_x, 6_y$ the betatron functions

Within this band a vertical ping would generate a coupled horizontal coherent oscillation of frequency $v_x - v_y$ and of amplitude:

$$\frac{\Delta b}{a} = \frac{1}{2(8s)(v_x - v_y)} \int_0^c \sqrt{6_x^2 s_y} \, kds$$

where Δb is the coupled amplitude horizontally
 a is the pinged amplitude vertically.

To distinguish between this effect and skew quadrupole components due to remnant and stray fields the experiment was performed at 150 GeV. With a tune split, $v_x - v_y = 0.1$, the coupled amplitude observed was 40% of that generated by the ping in its own plane and the oscillograms clearly showed the beat frequency $v_x - v_y$ (ten turns per wavelength for $v_x - v_y = 0.1$). These beats were of opposite phase in the two planes. Using above expression we calculated the angle of roll, about 8 milliradians, to be applied to 12 equally spaced quadrupoles to neutralise the coupling. This adjustment reduced the coupling effect by almost an order of magnitude.

We repeated the experiment at injection, correcting the average skew quadrupole component by adjusting twelve d.c. skew quadrupole magnets and we found we could eliminate the coupling even when $v_x - v_y$ was much less than 0.1.

4. Correction of Chromaticity

Magnetic measurements show that the MAF main ring dipole magnets have a remanent field whose predominant imperfection is a sextupole term. The field falls parabolically towards the edges of the poles. The average derivative is:

$$dB_y/dx^2 = 0.05 \text{ T m}^{-2}$$

This field distortion can be understood qualitatively if one remembers that flux lines in the iron yoked at the centre of the poles are longer than those from the edge. The remanent magnetomotive force, $\int H_c dl$, is larger near the pole centre.

The chromaticity in each phase plane produced by this sextupole shape is

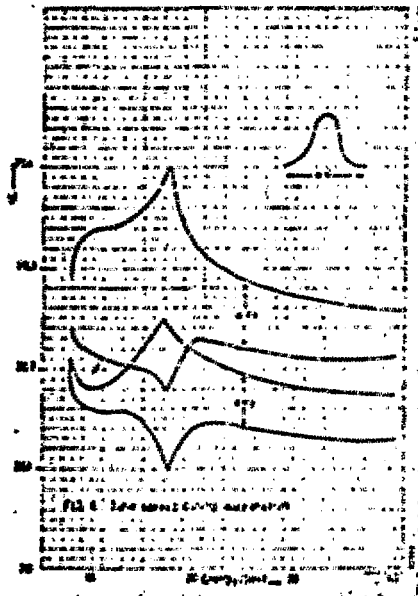
$$(dv/v)/(dp/p) = 9$$

seven times larger than that due to the momentum dependence of the focusing strength of the lattice. Uncorrected it would introduce a tune spread of $\Delta v = \pm 0.63$ for a momentum spread within the beam of $\pm 0.5\%$, measured by observing the time taken for the coasting injected beam to lose its 53 MHz r.f.

structure. The half widths quoted are those at the half height of the distributions.

During the early commissioning of the machine air cored sextupoles had been installed to correct this large chromaticity. These had been placed in all but a few of the short straight section spaces which follow each main ring quadrupole. Those near F quadrupoles and those near D quadrupoles should ideally have been separately powered to neutralise dv_x/dp and dv_y/dp independently but for practical reasons all sextupoles were in series and powered with a simple square pulse covering only the injection period and the parabola. They were therefore not ideal tools for accurate chromaticity control.

We measured the v spread in each plane at a number of points in the acceleration cycle by counting the number of machine revolutions that a pinged coherent betatron oscillation took to smear to half its original signal strength. For a Gaussian tune distribution the reciprocal of this number is a measure of the extreme (2 σ) spread in tune. Figure 4 shows the way in which the tune spread developed during the cycle. Starting



from almost perfect compensation in the vertical plane the chromaticity changes in each plane during the parabola as eddy current sextupole fields develop in the vacuum chamber. The momentum spread also swells, peaking at almost double its injection value in passing through transition. This further adds to Δv . The edges of the proton population cross the third and fourth order stopbands.

We therefore installed a new set of iron cored sextupoles with independent control of the set next to F quadrupoles and the set next to D quadrupoles. The currents in F and D sets are related to the dv_x/dp and dv_y/dp via a simple 2 x 2 matrix transformation which was built into the control software to give independent orthogonal control in the two planes.

The time development of sextupole imperfections contained three components: a steady one due to remanent fields, a component proportional to magnet excitation (B) and due to the geometry of the main ring dipoles and finally a component growing as dB/dt, generated by eddy currents in the vacuum chamber. We therefore powered the correctors with a current waveform:

$$I = a + \frac{bB}{dc} + cB$$

deriving the dB/dt and B signals from the main ring reference magnet.

Each of the coefficients, a, b, c multiplied by the 2 x 2 matrix could be controlled directly from a page on the main ring console display.

We set up each coefficient in turn at energies at which its influence predominates (3, 17 and 60 GeV), minimising the decay time of pinged betatron excitations and, repeating the tune spread experiments, we found $\Delta v \leq \pm 0.005$ throughout the acceleration cycle.

As expected beam survival improved as a result of this correction and the machine became much less sensitive to adjustments in the ratio of quadrupole to dipole current during the parabola.

5. Correction of Third Order Stopbands

Our early transmission experiments had revealed the strong influence of the four third order stopbands which intersect at $v = 20.33$ close to the nominal working point:

$$3v_x = 61, \quad \frac{1}{16} \frac{3^{3/2}}{4} (3^2 v_y / 2v_x^2) e^{i61\theta} \quad d_3$$

$$v_x + 2v_y = 61, \quad \frac{1}{16} \frac{3}{4} v_y (3^2 v_y / 2v_x^2) e^{i61\theta} \quad d_2$$

$$2v_x + v_y = 61, \quad \frac{1}{16} \frac{3^{3/2}}{4} (3^2 v_x / 2v_y^2) e^{i61\theta} \quad d_1$$

$$3v_y = 61, \quad \frac{1}{16} \frac{3^{3/2}}{4} (3^2 v_x / 2v_y^2) e^{i61\theta} \quad d_4$$

The table lists the resonances and their driving terms which are all 61st Fourier harmonics of the azimuthal pattern of sextupole imperfections weighted according to the local betatron functions. The first two resonances are driven and may be corrected by regular sextupoles with symmetry about a vertical plane; the same symmetry as one expects from the main ring dipoles. The last pair are driven by skew sextupoles of symmetry about the median plane. To correct all four stop bands one must use sextupole magnets of both regular and skew types.

The weighting factors are such that a further subdivision of correctors into those near F quadrupole locations where β_x is large and β_y small and those near D locations where the opposite is true gives one almost orthogonal control of each resonance.

To generate the correct phase and amplitude of the 61st harmonic and neutralise the driving term the current settings of the individually powered sextupoles were ganged up through the control system to increment the sine or cosine amplitude in the strength pattern.

Tuning the machine to sit exactly on one of the stopbands we could adjust the amplitudes of the sine and cosine components to achieve 70% transmission. A contour plot versus the two variables revealed a simple maximum.

We calculated the width of the stopband from the strength of the correctors. For a proton at the periphery of the beam (1 cm amplitude at $\delta = 100 \mu$) Δv is greater than ± 0.01 . We had expected these stopbands to be due to variations in the azimuthal pattern of the remanent sextupole fields responsible for the chromaticity. We know that the remanent fields in the dipole magnets constructed from unshuffled laminations varied by as much as $\pm 40\%$. Yet this could only account for a stopband $\Delta v = \pm 0.002$.

Clearly other, stronger sextupoles were present and we soon discovered that the uneven pattern of chromaticity correction sextupoles determined by the need to leave room in some short straight sections for other equipment contained driving terms of the appropriate magnitude and phase to explain the observed widths.

We redeployed these chromaticity sextupoles in a pattern considerably less rich in dist harmonic taking into account the differing weighting factors in the table and repeated our transmission scan. The line widths had clearly become very much smaller and this was reflected in an improvement from 1.8 to 1.4×10^{-11} in the intensity which could be accepted from the booster and accelerated to full energy.

We went on to compensate these much thinner resonances and from the corrector strength deduced a width commensurate with the theoretical estimate based on magnet measurements.

Our transmission scan showed all four lines to be comparable in width. We presume that sextupole fields of the skew configuration were present coming from assembly errors in the quadrupoles upon which we had little measurement data. We therefore installed F and D sets of skew sextupoles and set about compensating each of the four resonance lines scanning through each in turn along a line $v_x - v_y = 0.1$ where they are clearly resolved in the transmission scan. Figure 5 shows the effect of this compensation which raised the intensity which could be accepted and accelerated to a further 50%.

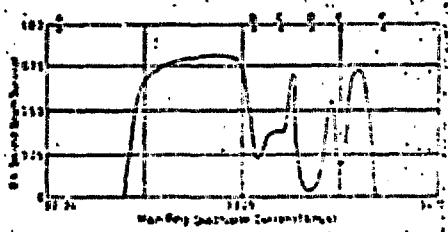
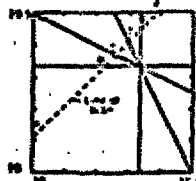


Fig. 5.13. Transmission Intensity versus Working Point Correction.

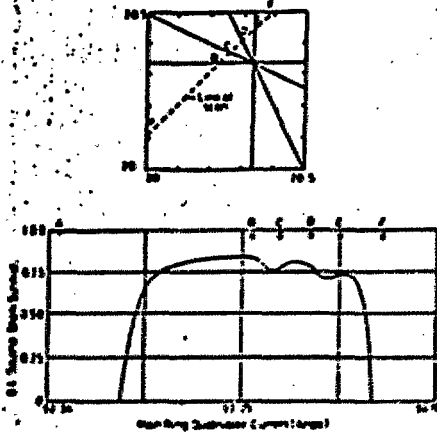


FIG. 5. Phase diagram and transmission characteristics.



Fig. 6 - Contour model of transmission.

Figure 6 shows a model of this diamond's contours with no harmonic correction applied. The integer has a width of $\Delta v = \pm 0.05$ compared with ± 0.1 in the original diamond. The region around 19.2 gives somewhat higher transmission and much more elbow room to accommodate changes in the working point due to magnet ripple and quadrupole power supply regulation. Accordingly, it was decided to change the operational working point permanently from 20.2 to 19.2 and improvement in accelerated beam has resulted.

Conclusions

These experiments demonstrated the deleterious effect of non-linear field imperfections in the guide field. It is apparent from transmission scans like Fig. 5 that beam survival is affected over a much wider band than the classical stopband width even when the measures have been taken to reduce the resonance and amplitude dependence of the tune. The reason for this line broadening is still being investigated. It may be due to ripple in the excitation of the dipole and quadrupoles.

As a result of these experiments and improvements the four dimensional acceptance of the main ring increased by almost an order of magnitude to match improvements in booster intensity and reduce the fraction of the beam lost after injection.

Yet even when the third order resonances had been corrected the acceptance was barely larger than the diameter of the booster beam. To enlarge this still further to be commensurate with the geometrical size of the vacuum chamber will require correction of fourth and higher order stopbands which are not resolved in transmission scans at injection but which we know are there from measurements at higher energy.

6. Compensation with Octupoles

Seeking to improve the linearity of the machine still further we measured the amplitude dependence of the tune by pinging coherent oscillations of a range of amplitudes and adjusting a set of d.c. series powered octupoles to make $\partial^2 v / \partial A^2$ zero. Zero harmonic octupole imperfections in the lattice also generate a curvature to the chromaticity $\partial^2 v / \partial p^2$. We measured the shape of $v(p)$ by pinging and steering to various mean radii with an r.f. bump. We optimized the octupoles to give a flat curve. Both techniques arrived at the same octupole strength. They proved effective in improving the tune spread. One could maintain coherent oscillations undiminished for several hundred turns indicating a Δv of a few $\times 10^{-4}$. Not surprisingly the machine became so linear at this point that a resistive wall instability emerged. The diagnosis and cure of this instability is the subject of another paper in this conference.

7. Alternative Working Point

The definition of our resonant scans had improved sufficiently by this time that we were able to construct three dimensional models of the transmission over the diamond: $20 < v_x, v_y < 20.5$ and could identify the valleys of the third integer resonances as well as less well defined depressions at the location of fourth and higher order resonances.

The integer stopbands $v_x, v_y = 20$ were very wide and we suspected that one of their main components was the systematic resonance

$$3v = 60 = 10 S$$

where S is the superperiodicity of the long straight sections and hence of the systematic sextupole imperfection.

Such systematic relations reoccur at all even v values for $S = 6$ and give rise to very wide stopbands. We therefore decided to explore the diamond just above 19 to see if the integer was less strong.